Proc. Natl. Acad. Sci. USA
Vol. 92, pp. 8239–8243, August 1995
Biophysics

Determination of the distance between two spin labels attached to a macromolecule

(biradicals/electron paramagnetic resonance)

MARK D. RABENSTEIN AND YEON-KYUN SHIN†

Department of Chemistry, and Division of Structural Biology, Lawrence Berkeley Laboratory, University of California, Berkeley, CA 94720

Communicated by Sung-Hou Kim, University of California, Berkeley, CA, April 10, 1995

ABSTRACT **An EPR "spectroscopic ruler" was developed using a series of α-helical polypeptides, each modified with two nitroxide spin labels. The EPR line broadening due to electron–electron dipolar interactions in the frozen state was determined using the Fourier deconvolution method. These dipolar spectra were then used to estimate the distances between the two nitroxides separated by 8–25 Å. Results agreed well with a simple α-helical model. The standard deviation from the model system was 0.9 Å in the range of 8–25 Å. This technique is applicable to complex systems such as membrane receptors and channels, which are difficult to access with high-resolution NMR or x-ray crystallography, and is expected to be particularly useful for systems for which optical methods are hampered by the presence of light-interfering membranes or chromophores.**

Many studies in structural biology are dependent on the physical techniques to measure distances in proteins and nucleic acids. X-ray crystallography and high-resolution NMR have been useful in determining the three-dimensional structures of relatively simple biological macromolecules. For complex systems such as membrane proteins, fluorescence energy transfer (FET) has been the main alternative for measuring distances up to 80 Å. FET has been successful for studies of intermolecular organization in biological systems (1, 2), ligand–receptor interactions (3), and structures of nucleic acids (4).

Recently, site-directed spin labeling EPR has become useful for studying proteins (5, 6). One or two native residues are mutated to cysteines, which are then labeled with thiol-specific nitroxide spin labels. This technique can also be used to study local secondary structure (7, 8). Nucleic acids also appear to be amenable to spin labeling (9). Although spin labeling has been used to estimate distances in the past (10–12), no EPR "spectroscopic ruler" similar to that developed by Stryer and Haugland (13) for FET has been constructed or tested on model systems.

In this work a convenient and accurate EPR method to determine distances between two site-specifically placed nitroxides in the range of 8–25 Å in biomacromolecules is presented. In this method the pure dipolar spectrum for two interacting spins in the frozen state is directly Fourier deconvoluted from the dipolar broadened continuous-wave EPR spectrum. The average interspin distance and the variance of its distribution are obtained from this dipolar spectrum.

The method was tested using α-helical peptides as a model system. The peptides were alanine-based helices with spin-labeled cysteines substituted for alanines at two locations from 1 to 13 residues apart. There is excellent agreement between the spin–spin distances from a simple model and experimental results in the range of 8–25 Å. It is also shown that this method is useful for systems that have impurities of singly labeled species. Although this methodology is complementary to FET, EPR has the advantages of easier sample preparation and higher precision and the disadvantage of requiring low temperature conditions.

The publication costs of this article were defrayed in part by page charge payment. This article must therefore be hereby marked "*advertisement*" in accordance with 18 U.S.C. §1734 solely to indicate this fact.

THEORY

Dipolar Interactions. In the motionally frozen state, two unpaired electrons separated by the distance r are coupled to each other through electron-electron dipolar and other short-range interactions such as J coupling. When $r \geq 8$ Å, the dipolar interactions dominate (see *Discussion*). The EPR absorption lines are then split by 2B in the magnetic field (12, 14):

$$2B = \left(\frac{3}{2}\right) g_e \beta (3\cos^2\theta - 1)/r^3, \quad [1]$$

where g_e is the isotropic g value of the electrons, β is the electron Bohr magneton ($\frac{3}{2} g_e \beta = 30.3$ G·Å^3), and θ is the angle between the interspin vector and the external magnetic field. Here we assume that the effect of anisotropic magnetic tensors is negligible (15).

In most biological systems the distribution of θ is isotropic (12). Moreover, for a given θ, both nitroxide hyperfine magnetic tensors are expected to be isotropically distributed due to the axial rotational degree of freedom along the interspin axis and the flexible link between the nitroxide groups and the rest of the peptide. Thus, a powder-pattern EPR spectrum is expected for an ensemble of spin pairs with the given angle θ in the absense of the dipolar interactions. It is then possible to treat the EPR spectrum of two interacting spins as convolution of the noninteracting powder-pattern absorption spectrum with a dipolar broadening function D(r, B) (Fig. 1), known as a Pake pattern (16). The average splitting ⟨2B⟩ over the distribution D(r, B) is then:

$$\langle 2B \rangle = (0.75)\left(\frac{3}{2}\right) g_e \beta / r^3. \quad [2]$$

Thus, the EPR spectrum Π(B) for the two nitroxides is described by:

$$\Pi(B) = \int_{-\infty}^{\infty} S(B') D(r, B' - B) dB', \quad [3]$$

where S(B) is the noninteracting EPR spectrum (16, 17). However, in practice there will be a distribution of interspin distances due to the tethering of the nitroxide side chain as well as the conformational variation of the macromolecules. In this situation the EPR spectrum is describe by:

Abbreviation: FET, fluorescence energy transfer.

†To whom reprint requests should be addressed.

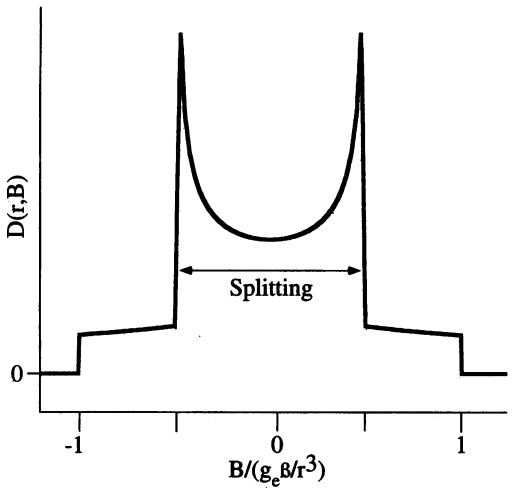

FIG. 1. A "Pake pattern" dipolar broadening function.

$$\Pi(B) = \int_{-\infty}^{\infty} S(B')M(B' - B)dB', \quad [4]$$

where M(B) is the weighted sum of the D(r, B) over the distribution of the distances P(r):

$$M(B) = \sum_r P(r)D(r, B). \quad [5]$$

Fourier Deconvolution. Since Π is simply a convolution of S and M in real space, Eq. **4** is simplified in Fourier space using the convolution theorem (18):

$$\Pi^*(\varpi) = S^*(\varpi)\cdot M^*(\varpi), \quad [6]$$

where the superscript * indicates the Fourier-transformed functions and ϖ is the inverse variable of B in units of G^{-1}. M(B) is then obtained from the inverse Fourier transform of the division of Π^* by S*:

$$M(B) = \frac{1}{\sqrt{2\pi}}\int_{-\infty}^{\infty} \exp(2\pi i\varpi B)\frac{\Pi^*(\varpi)}{S^*(\varpi)}d\varpi. \quad [7]$$

Thus, the average splitting $\langle 2B\rangle$ for a given P(r), and subsequently the average separation of the two nitroxides, is obtained from:

$$\langle 2B\rangle = \int_{-\infty}^{\infty} |2B|\cdot M(B)dB / \int_{-\infty}^{\infty} M(B)dB \quad [8]$$

and

$$\langle r\rangle = \left(0.75\left(\frac{3}{2}\right)g_e\beta/\langle 2B\rangle\right)^{\frac{1}{3}}. \quad [9]$$

The variance S_r of P(r) is also calculated from M(B):

$$S_r = \frac{5}{4}\int_{-\infty}^{\infty} (2B)^2M(B)dB / \int_{-\infty}^{\infty} M(B)dB - \left(\frac{4}{3}\right)^2\langle 2B\rangle^2. \quad [10]$$

Here, the coefficient 5/4 is a correction factor for averaging of $(2B)^2$ over the Pake patten D(r, B) (Fig. 1), analogous to Eq. **2** for $\langle 2B\rangle$.

Monoradical Impurities. For practical purpose, monoradical impurities due to the incomplete spin labeling reaction are a potential problem when analyzing spin–spin interactions. EPR spectra with monoradical contamination can be incorrectly interpreted as larger nitroxide–nitroxide separation. The Fourier deconvolution method can, in principle, separate the dipolar spectrum for the interacting nitroxides from the spectral contribution from the monoradical contaminants. The composite EPR spectrum for a mixture of mono- and biradicals is given by:

$$\Pi(B) = a\int_{-\infty}^{\infty} S(B')M(B' - B)dB' + b\cdot S(B), \quad [11]$$

where a is the fraction of the biradical and b is the fraction of monoradicals with a + b = 1. Thus, after Fourier deconvolution we obtain:

$$M'(B) = aM(B) + b\delta(0) \quad [12]$$

and the "contaminating" δ-function contribution is readily removed, yielding the pure dipolar spectrum.

MATERIALS AND METHODS

Peptide Synthesis and Labeling. To test the method, alanine-based α-helical peptides were synthesized (8, 19, 20). In 20 mol % trifluoroethanol, these are known to be α-helices. We made a series of variants of these peptides changing two alanines to cysteines with various separations, as shown in Table 1.

Peptides were synthesized on an ABI 430A peptide synthesizer using 9-fluorenylmethoxycarbonyl-protected amino acids and Rink amide 4-methyl benzhydrylamine resin (Nova Biochem). They were capped with acetic anhydride. After cleavage crude peptides were purified by reversed-phase HPLC on C_{18} resin using a gradient of 15–40% acetonitrile in 0.1% trifluoroacetic acid, frozen immediately, and then lyophilized. Purified peptides were labeled with a 4-fold excess of methanethiosulfonate spin label (Reanal, Hungary) for 1.5 hr in 20 mM Mops (pH 6.9) and then repurified as described above. Masses of the labeled and unlabeled peptides were verified by electrospray mass spectrometry. Following EPR measurements, the samples were rechecked by HPLC to ensure the purity of samples.

EPR Measurements. EPR spectra were taken with a Bruker ESP 300 E EPR spectrometer equipped with a loop-gap resonator (Medical Advances, Milwaukee, WI). Spectra were taken at 150 ± 2 K with a modulation amplitude of 0.66 G and a peptide concentration of 0.8–1 mM. Spectra were independent of concentration in the range of 20 μM to 1.5 mM.

RESULTS

EPR Spectra. As expected, EPR spectra of doubly labeled variants (Fig. 2, spectra b–j) are all broader than the spectrum of a singly labeled one (Fig. 2, spectrum a), and the extent of

Table 1. Amino acid sequences of spin-labeled peptides

4K	Ac-AAAAKAAAAKAAAAKAAAAKA-NH_2
4K-(6)	.....C.....
4K-(6, 7)	.....CC.....
4K-(6, 8)	.....C.C.....
4K-(6, 9)	.....C..C.....
4K-(4, 8)	...C...C.....
4K-(4, 9)	...C....C.....
4K-(6, 12)	.....C.....C.....
4K-(4, 11)	...C......C.....
4K-(4, 13)	...C.........C.....
5K-(4, 17)	...C.............C....AAAKA-NH_2

Ac, acetyl; A, alanine; C, cysteine; K, lysine; "." same as 4K.

broadening is clearly dependent on the spatial separation of nitroxides. A well-defined α-helix has 3.6 residues per turn, and thus residues three apart or four apart along the sequence (i, $i + 3$) or (i, $i + 4$) are spatially very close, while residues one or two apart, (i, $i + 1$) or (i, $i + 2$) are far apart, where (i, j) corresponds to the peptide with nitroxides at ith and jth positions. Consistent with this ranking of the spatial separations between a pair of nitroxides in each peptide, the spectra of 4K-(4, 8) and 4K-(6, 9) are broader than those of 4K-(6, 7) and 4K-(6, 8).

Dipolar Broadening Function. All EPR spectra were analyzed according to Eqs. **6–8** using fast Fourier transform routines (18). Both real and imaginary components of a dipolar spectrum in Fourier space $[\Pi^*(\varpi)/S^*(\varpi)]$ contain high-amplitude noise at high values of ϖ (Fig. 3). They were suppressed by applying a square filter function $[f(\varpi) = 1$ for $\varpi < \kappa$, and $f(\varpi) = 0$ for $\varpi \geq \kappa]$ in the analysis. In fact, a sudden increase of noise at high ϖ makes it trivial to objectively determine the cutoff value κ. We also found that the dipolar spectrum is not very sensitive to some variation of κ. The final dipolar spectrum (Fig. 4) was obtained by averaging over a small range of κ values. The distribution $P(r)$ of interspin distance leads to broadening functions that are the sum of many Pake patterns. This, in combination with the EPR linewidth, leads to broadening funtions that do not look like Pake patterns.

Spin–Spin Distances. The average distance and the variance were calculated for each peptide using Eqs. **9** and **10**. The results are plotted vs. distances calculated based on the α-helical geometry in Fig. 5. The theoretical nitroxide–nitroxide separation for each doubly labeled variant was

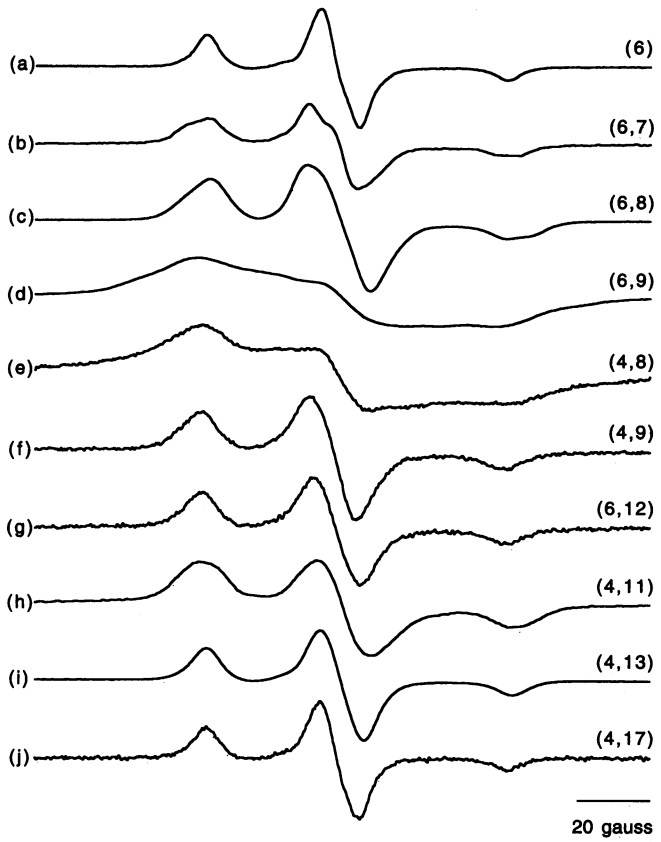

FIG. 2. Spectrum a: First derivative EPR spectrum of the singly labeled peptide. Spectra b–j: EPR spectra of peptide biradicals. EPR spectra were taken at 150 ± 2 K with a modulation amplitude of 0.66 G. The peptide concentration was in the range of 0.5–1 mM in 20 mM Mops buffer containing 20 mol % TFE trifluoroethanol (pH 7.1). In this condition the peptides are known to be α-helices (16–18).

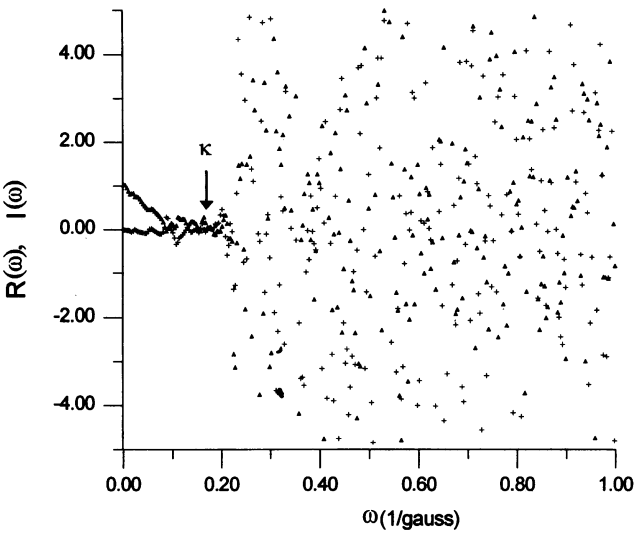

FIG. 3. Real $R(\varpi)$ (▲) and imaginary $I(\varpi)$ (+) parts of the dipolar broadening function for 4K-(6, 12) in Fourier space.

calculated assuming that the peptide is a rigid α-helix of a 5.41-Å pitch and 1.50-Å translation per residue (21). Because the exact side-chain conformations are unknown, the distance between the helix axis and the radical, known as the "arm length," is unknown. The "arm" is assumed to be the line perpendicular to the helix axis intersecting the cysteine β-carbon. Spin label separations were calculated for various arm lengths and compared to the experimental data. An arm length of 6.7 Å best fit the experimental data. There is good agreement between the experimental values and the theoretical values, with a standard deviation of 0.9 Å for the entire range of 7.5–25 Å. Furthermore, it should be noted that with spin labels 7 residues apart, the nitroxides are nearly eclipsed. Thus, their separation is almost independent of the assumed arm length. For example, the separation is calculated to be 10.6 Å for an arm length of 4 Å (corresponding to the position of the β-carbon) and 11.6 Å for an arm length of 13 Å (corresponding to a completely extended spin label). These are both close to the measured value of 10.5 Å.

Monoradical Impurities. To test the validity of Eq. **12** we mixed the singly labeled with doubly labeled peptides [4K-(6) and 4K-(4, 8)] in a molar ratio of 2:1. The composite spectrum of the mixture is shown in Fig. 6*a*. The broadening function $M'(B)$ obtained from Fourier deconvolution (Fig. 6*b*) is a mixture of a broad component, which is similar to the dipolar spectrum of 4K-(4, 8) in Fig. 4, and a sharp component centered at the origin, which corresponds the δ function in Eq.

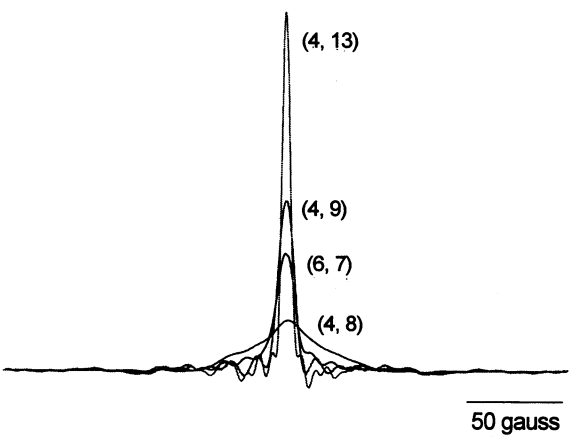

FIG. 4. Fourier deconvoluted dipolar broadening functions.

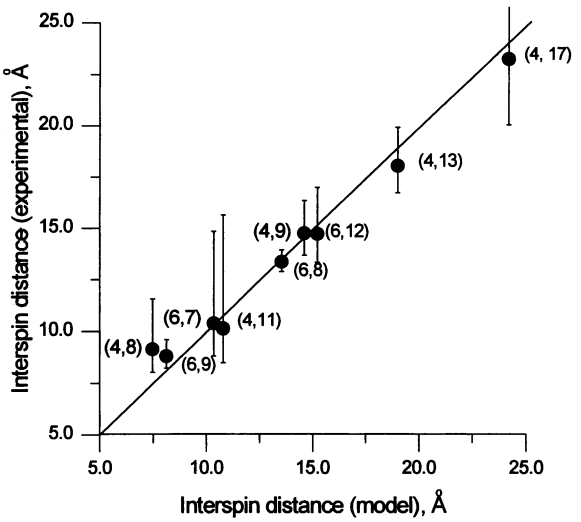

FIG. 5. Nitroxide–nitroxide separations: Experiment vs. model. The theoretical nitroxide–nitroxide separation for each peptide was calculated assuming that the peptide is a rigid α-helix of a 5.41-Å pitch and 1.50-Å translation per residue (21). The nitroxide side chain is assumed to be extended along the line connecting the central helical axis and the β-carbon in cysteine. In this geometrical model the paramagnetic center in the nitroxide moiety is located at 6.7 Å from the center of the helix. The standard deviation of the experiment from the model is 0.9 Å.

12. Thus, the true dipolar spectrum can be separated from M′(B) at least in cases of the small interspin separations. The estimated spin–spin distance from the broad component was the same as that of 4K-(4, 8) within experimental error.

DISCUSSION

The Fourier deconvolution method is based on the assumption that the biradical spectrum is the convolution of the dipolar broadening function and the monoradical spectrum. This assumption may have to be confirmed by an extensive theoretical treatment. However, we anticipate that this would be nontrivial since we have no *a priori* knowledge of the actual angular distribution of magnetic tensors at a given θ (see Eq. 1). However, the good agreement between experiment and theory (Fig. 5) suggests that the convolution is a good empirical approximation for the practical use of the method.

The maximum distance that this method can measure is ≈25 Å, which is set by the intrinsic linewidth of the continuous-wave EPR spectrum. Use of deuterated spin labels may increase the limit by reducing the inhomogeneous broadening. Another approach to extend the measurable distance would be to use time domain EPR techniques (22, 23). For current model systems the resolution of the measurement calculated from the variances is 2.2 Å, close to the value (1.8 Å) obtained from the molecular dynamics calculation (7). This is perhaps mostly due to the tethering of the nitroxide side chain, provided that the backbone of the helix is fixed.

When the interspin distance is very small, the EPR line shape may become complicated due to the short-range interactions such as *J* coupling and the magnetic anisotropy (15, 24). Despite several attempts to elucidate these matters, it is unclear how they affect the EPR line shape at very short distances in the frozen state. On the other hand, the good agreement between experiment and theory (Fig. 5) suggests that the simple analysis assuming only the dipolar interactions is a reasonable and practical approximation when the interspin distance is longer than ≈8 Å.

The doubly labeled peptides have at least 17 bonds separating two electrons so that the through-bond spin–spin interaction is not significant. The biradical 4K-(6, 7), with 17 bonds separating the electron spins, shows less broadening than 4K-(4, 11), which has 35 bonds separating the electrons. Thus, the line broadening in spectra depicted in Fig. 2 must be predominantly due to through-space interactions.

In practice, the magnetic tensors may be slightly different for two nitroxides due to the differences in the polarity of surroundings: for example, one nitroxide (N_1) is in the hydrophobic region and the other (N_2) is exposed to the solvent. Since the dipolar spectrum M(B) is expected to be the same for N_1 and N_2, it is only necessary to use $\{S_1(B) + S_2(B)\}/2$ in place of S(B) to calculate M(B) using Eqs. **6** and **7**. Experimentally, $S_1(B)$ and $S_2(B)$ can be determined by singly labeling the system at position 1 or 2, respectively.

The EPR method and FET should be comparable and complementary for the distance range of 8–25 Å. We wish now to consider comparisons of the EPR method with FET. First, the chemistry of spin labeling is much simpler than that of fluorescence labeling. This is because EPR uses the same spin label for the two sites of interest, while FET requires heterogeneous labeling, donor to one site and acceptor to the other. In addition, recent progress in site-specific spin labeling techniques (5, 6) makes the EPR method promising for many biologically interesting systems. Application of FET to biological systems is often problematic because of light-absorbing chromophores and light-absorbing and -scattering membranes. The EPR method, however, does not require the light trans-

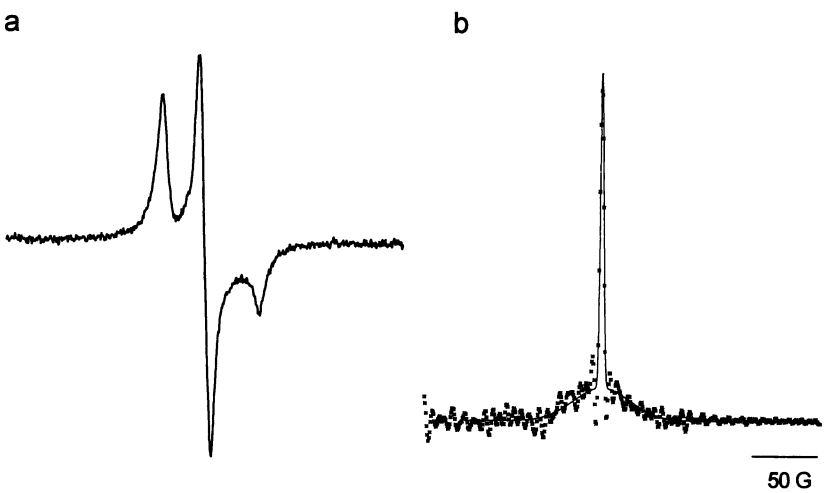

FIG. 6. (*a*) EPR spectrum for the mixture of 4K-(4, 8) and 4K-(6) in the ratio of 1:2. (*b*) Corresponding dipolar broadening function.

parency, rendering wide applicability. Moreover, the nitroxides are much smaller than the fluorescent groups and contain a well-localized paramagnetic center. Furthermore, FET analysis can be complicated due to incomplete averaging of the relative orientation of the donor and the acceptor in the time scale of the FET (25) (cf. κ^2), often resulting in inaccurate measurements. Thus, higher precision is expected for the EPR method.

One major drawback of the EPR method is that it requires the motionally frozen sample. Thus, this method may not be adequate for the real-time detection of the functionally important conformational changes of macromolecules. Alternatively, however, the EPR method can be combined with freeze-quench techniques (26, 27) to follow time-dependent conformational changes of proteins. FET is somewhat advantageous for time-resolved studies since it does not require frozen samples.

In summary, the Fourier space analysis method to estimate the interspin distance between the two interacting nitroxides through the dipolar interaction was tested for a model system. It has been shown that this method accurately measures the interspin distance in the range of 8–25 Å. The accurate determination of distances in this range may be crucial for the understanding of mechanisms of signal transduction or energy transduction involving subtle structural rearrangements (28, 29). This method certainly opens up a new area for the investigation of important biological phenomena.

We thank Prof. S.-H. Kim for discussion and Dr. D. King for mass spectrometry. This research was supported by American Chemical Society Grant PRF 28160-G7 and National Institutes of Health Grant GM51290-01.

1. Langloise, R., Lee, C., Cantor, C., Vince, R. & Pestka, S. (1976) *J. Mol. Biol.* **106,** 297–313.
2. Fairclough, R. & Cantor, C. (1977) *Methods Enzymol.* **48,** 347–379.
3. Carraway, K. & Cerione, R. (1993) *Biochemistry* **32,** 12039–12045.
4. Clegg, R. M., Murchie, A. I., Zechel, A., Carlberg, C., Diekmann, S. & Lilley, D. M. (1992) *Biochemistry* **31,** 4846–4856.
5. Altenbach, C., Marti, T., Khorana, H. G. & Hubbell, W. L. (1990) *Science* **248,** 1088–1092.
6. Shin, Y.-K., Levinthal, C., Levinthal, F. & Hubbell, W. L. (1993) *Science* **259,** 960–963.
7. Miick, S. M., Martinez, G. V., Fiori, W. R., Todd, A. P. & Millhauser, G. L. (1992) *Nature (London)* **359,** 653–655.
8. Fiori, W. R., Miick, S. M. & Millhauser, G. L. (1993) *Biochemistry* **32,** 11957–11962.
9. Bobst, A. (1979) in *Spin Labeling II: Theory and Applications*, ed. Berliner, L. J. (Academic, New York), pp. 291–346.
10. Anthony-Cahill, S. J., Benfield, P. A., Fairman, R., Wasserman, Z. R., Brenner, S. L., Stafford, W. F., Altenbach, C., Hubbell, W. L. & DeGrado, W. F. (1992) *Science* **55,** 979–983.
11. Eaton, G. & Eaton, S. (1989) in *Biological Magnetic Resonance*, eds. Berliner, L. & Reubens, J. (Academic, New York), Vol. 8, pp. 339–397.
12. Likhtenshtein, G. I. (1976) *Spin Labeling Methods in Molecular Biology* (Wiley, New York).
13. Stryer, L. & Haugland, R. P. (1967) *Proc. Natl. Acad. Sci. USA* **58,** 719–726.
14. Ciecierska-Tworek, Z., Van, S. P. & Griffith, O. H. (1973) *J. Mol. Struct.* **16,** 139–148.
15. Boas, J., Hicks, P. & Pilbrow, J. (1978) *J. Chem. Soc. Faraday Trans. 2* **74,** 417–431.
16. Pake, G. E. (1948) *J. Chem. Phys.* **16,** 327–336.
17. Abragam, A. (1961) *The Principles of Nuclear Magnetism* (Oxford Univ. Press, New York).
18. Press, W., Teukolsky, S., Vetterling, W. & Flannery, B. (1992) *Numerical Recipes in C* (Cambridge University, Cambridge, U.K.), pp. 538–543.
19. Marqusee, S., Robbins, V. H. & Baldwin, R. L. (1989) *Proc. Natl. Acad. Sci. USA* **86,** 5286–5290.
20. Lockhart, D. J. & Kim, P. S. (1993) *Science* **260,** 198–202.
21. Creighton, T. E. (1983) *Proteins* (Freeman, New York).
22. Milov, A., Ponomarev, A. & Tsvetkov, Y. (1984) *Chem. Phys. Lett.* **110,** 67–72.
23. Larsen, R. & Singel, D. (1993) *J. Chem. Phys.* **98,** 5134–5146.
24. Closs, G., Forbes, M. & Piotrowiak, P. (1992) *J. Am. Chem. Soc.* **114,** 3285–3294.
25. Dale, R. E., Eisinger, J. & Blumberg, W. E. (1979) *Biophys. J.* **26,** 161–194.
26. Varley, P., Gronenborn, A. M., Christensen, H., Wingfield, P. T., Pain, R. H. & Clore, G. M. (1993) *Science* **260,** 1110–1113.
27. Subramaniam, S., Gerstein, M., Oesterhelt, D. & Henderson, R. (1993) *EMBO J.* **12,** 1–8.
28. Milburn, M. V., Prive, G. G., Milligan, D. L., Scott, W. G., Yeh, J., Jancarik, J., Koshland, D. E., Jr., & Kim, S. H. (1991) *Science* **254,** 1342–1347.
29. Milligan, D. L. & Koshland, D. E., Jr. (1991) *Science* **254,** 1651–1654.